

Electronic supplementary information

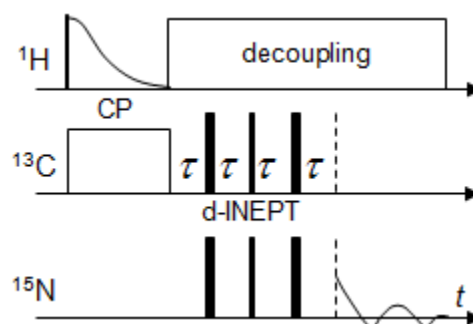
Experimental strategies for ^{13}C - ^{15}N dipolar NMR spectroscopy in liquid crystals at the natural isotopic abundance

Lukas Jackalin, Boris B. Kharkov, Andrei V. Komolkin, Sergey V. Dvinskikh

1. Phase cycles for the pulse sequences.

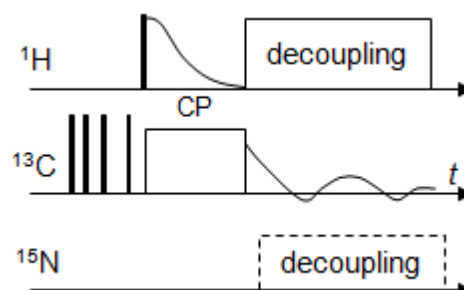
^{13}C - ^{15}N d-INEPT with ^1H - ^{13}C CP

^1H 90° pulse:	8(x), 8(-x)
^1H CP pulse:	y
^{13}C CP pulse:	y
^{13}C INEPT pulses:	$\phi_1 = x, -x$ $\phi_2 = 4(x), 4(y), 4(-x), 4(-y)$ $\phi_3 = 2(x, -x), 2(y, -y)$
^{15}N INEPT pulses:	$\phi_4 = x, -x$ $\phi_5 = 2(y), 2(-y)$ $\phi_6 = x, -x$
Receiver:	2(x), 2(-x), 2(y), 2(-y)



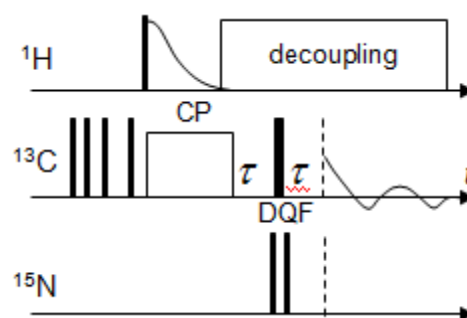
Carbon-13 difference spectra without and with nitrogen-15 decoupling in alternated scans

^1H 90° pulse:	4(x, x, -x, -x)
^1H CP pulse:	x
^{13}C CP pulse:	4(x), 4(-x), 4(y), 4(-y)
Receiver:	x, -x, -x, x, -x, x, x, -x, y, -y, -y, y, -y, y, y, -y



Carbon-13 spectra with heteronuclear ^{13}C - ^{15}N DQF

^1H 90° pulse:	4(x), 4(-x)
^1H CP pulse:	y
^{13}C CP pulse:	8(y), 8(-y)
^{13}C DQF pulse:	x
^{15}N DQF pulses:	$\phi_1 = x, -x$ $\phi_2 = 2(x), 2(-x)$
Receiver:	x, -x, -x, x, -x, x, x, -x, -x, x, x, -x, x, -x, -x, x



2. Simulated dipolar spectra for the pulse sequences of Fig. 1c.

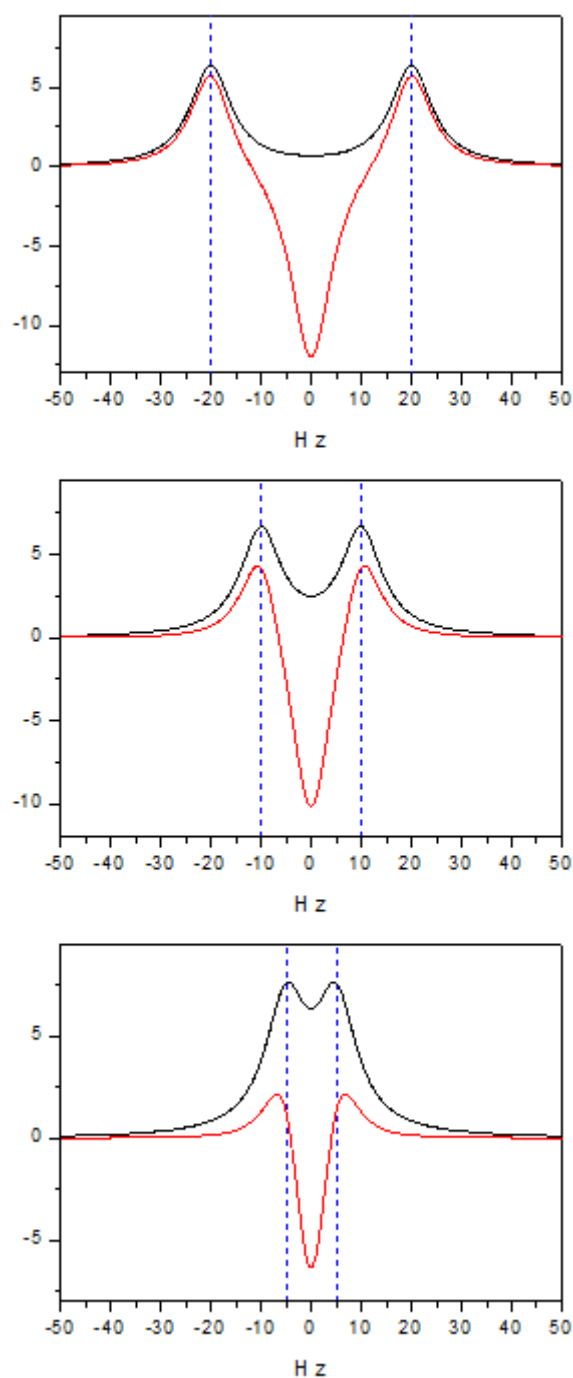


Fig. S1. Simulated dipolar spectra for the pulse sequences of Fig. 1c with dipolar coupling constant 20, 10 and 5 Hz (top to bottom) and lorentzian line broadening of 10 Hz. Red and black lines present spectra obtained without and with compensating scan, respectively.

Simulated spectra without compensating scan demonstrate that the intensity of the lines presenting dipole-split doublet is decreasing (positive peaks in red spectra) when dipole constant is comparable to line width. Moreover, apparent splitting (measured as the distance between peak maxima) becomes larger due to broadening effect. These artefacts are suppressed in the spectra measured with compensating scan (black lines). The numerical simulation was performed using Spinach programs (<http://spindynamics.org/Spinach.ph>).

3. Magnitude vs phase-sensitive DQF spectrum.

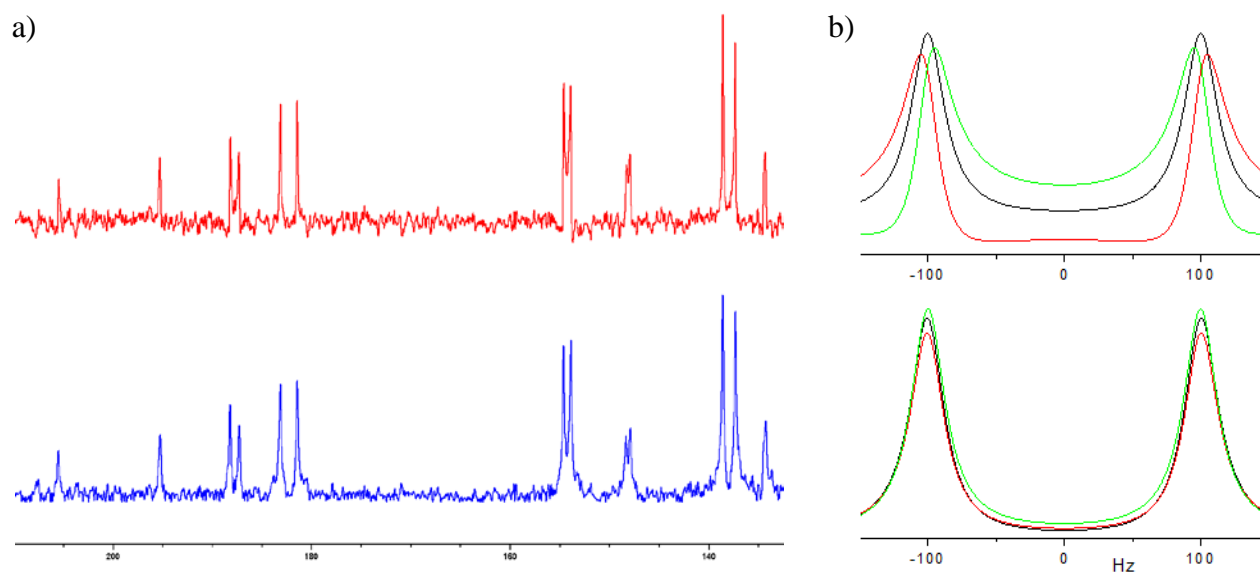


Fig. S2. (a) Fourier transform ^{13}C - ^{15}N DQF spectrum of MBBA processed in phase sensitive (red) and magnitude mode (blue). Spectrum was obtained by pulse sequence of Fig. 1d, 4k scans were accumulated. (b) Simulated DQF spectra processed in phase sensitive (top) and magnitude mode (bottom): $d_{CN} = 100$ Hz, line broadening 30 Hz, $\tau = 2500$ (black), 3000 (red), and 2000 μs (green).

In the magnitude mode spectrum, phase distortions, observed in phase sensitive spectra, are suppressed and the dipolar splittings are more accurately determined.

4. DFT data for sample BAB

Distances r_{CN} and angles $\theta_{CN,Z}$ were calculated from the BAB molecular geometry obtained by the DFT B3LYP/6-311+g(d) method in vacuo.

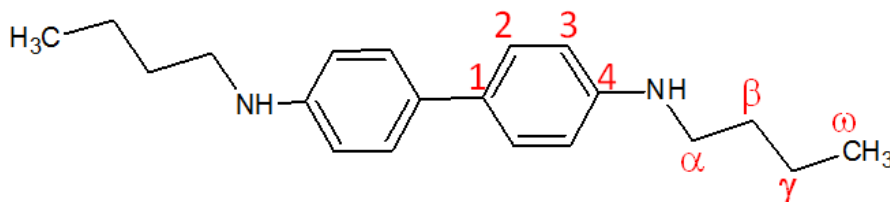


Table S1. ^{13}C - ^{15}N distances (Å), angles (degrees), and magnitudes of the dipolar couplings (Hz) in BAB.

Carbon	r_{CN}	b_{CN}	$\theta_{CN,Z}$	$ D_{CN} $
C4	1.39	-1140	2.2	660
C3	2.435	-212	29.5	77.9
C2	3.71	-60	19.0	29.3
C1	4.25	-40	0	23.2
C α	1.45	-1005	57.0	32.0
C β	2.46	-206	21.0	96.5
C γ	3.83	-54.5	33.5	17.2
C ω	5.01	-24.3	21.0	11.4

$$b_{CN} = -(\mu_0 / 8\pi^2)(\gamma_C \gamma_N \hbar / r_{CN}^3)$$

$\theta_{CN,Z}$ is the angle between the C-N vector and the molecular frame axis Z

$$D_{CN} \approx b_{CN} S_{ZZ} (3 \cos^2 \theta_{CN,Z} - 1) / 2$$

$$S_{ZZ} = 0.58$$

5. MD simulation of MBBA

Trajectories of the MD computer simulation of nematic MBBA have been calculated in previous work.¹ Here we only summarize essential details. Two models of the MBBA molecules were used: (1) fully atomistic model (FA) which takes into account all atoms in the molecule with force field OPLS-AA² and (2) a model of united atoms (UA) which joins hydrogen atoms with the adjacent heavy atoms (carbons) with force field OPLS.³ Multiscale transition method (MuScaT) was used to replace UA molecules with FA molecules.⁴ Analysis of the system during two time intervals 5.0-6.6 ns and 11.6-13.2 ns was performed by the FA model. During the initial and intermediate intervals the system was simulated by the UA model to speed-up the evolution of the system.

Simulated system was composed of 726 molecules placed in a cubic cell with periodic boundary conditions. Electrostatic interactions were calculated with Ewald method.⁵ Both force fields take into account intramolecular energies of conformational transitions: bond angle bending, torsional rotation, Van der Waals and electrostatic interactions of non-bonded atoms. Bond lengths were fixed with SHAKE algorithm.⁶ The other essential parameters were as follows: ensemble NVT; length of the cubic cell $L = 68.207 \text{ \AA}$; density of the substance $\rho = 1.0144 \text{ g/cm}^3$ which led to the mean value of pressure $p = 1 \text{ atm}$ within NVT ensemble; temperature $T = 307 \text{ K}$; thermostat Nose-Hoover algorithm^{7, 8} with time of reaction 0.504 ps; time step of simulation $\Delta t = 1 \text{ fs}$ and 2 fs for FA and UA models, respectively; cut-off radius $R_{\text{cutoff}} = 14.5 \text{ \AA}$; parameters for the Ewald sum $\alpha = 0.27 \text{ \AA}^{-1}$, $k = 7$.

For every molecule on each time step the following values were calculated: orientation of molecular frame XYZ in the laboratory frame xyz and the orientation of the director of liquid crystal in the laboratory frame, order parameter S_{ZZ} and biaxiality $S_{XX}-S_{YY}$ with respect to director, dipolar couplings in molecular frames. Averaging of dipolar couplings over all molecules on each step and over all time steps was performed. Obtained parameters are collected in the Table S2.

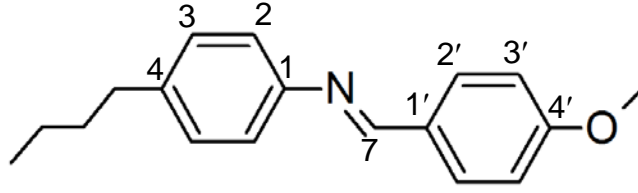


Table S2. ^{13}C - ^{15}N distances (Å), angles (degrees) and magnitudes of the dipolar couplings (Hz) in MBBA calculated from the MD trajectory.

Carbon	$\langle r_{CN} \rangle$	$\langle b_{CN} \rangle$	$\langle \theta_{CN,Z} \rangle$	$\langle D_{CN} \rangle$	$ D_{CN} ^*$
C1	1.340	1272	8.495	817	694
C2	2.357	234	28.231	92	78
C3	3.631	64	17.799	34	29
C4	4.135	43	7.920	28	24
C7	1.200	1771	49.541	106	90
C1'	2.322	245	19.459	127	108
C2'	2.822	137	11.837	54	46
C3'	4.210	41	10.512	20	17
C4'	4.998	25	7.860	15	13

$\langle r_{CN} \rangle$ is average distance

$$\langle b_{CN} \rangle = -\frac{\mu_0}{8\pi^2} \gamma_C \gamma_N \hbar \left\langle \frac{1}{r_{CN}^3} \right\rangle$$

$\langle \theta_{CN,Z} \rangle$ is the average angle between the C-N vector and the molecular frame axes Z

$$\langle D_{CN} \rangle = -\frac{\mu_0}{8\pi^2} \gamma_C \gamma_N \hbar \left[S_{ZZ} \left\langle \frac{3\cos^2 \theta_{CN,Z} - 1}{2r_{CN}^3} \right\rangle + (S_{XX} - S_{YY}) \left\langle \frac{\cos^2 \theta_{CN,X} - \cos^2 \theta_{CN,Y}}{2r_{CN}^3} \right\rangle \right]$$

$\theta_{CN,\alpha}$ is the angle between the C-N vector and the molecular frame axes $\alpha=X,Y,Z$

Molecular orientational order $S_{ZZ} = 0.664$

Biaxiality parameter ($S_{XX} - S_{YY}$) = -0.056

$$D_{CN}^* = 0.85 \langle D_{CN} \rangle$$

1. V. S. Neverov, A. V. Komolkin and T. G. Volkova, *Vestn. S.-Peterb. Univ., Ser. 4: Fiz., Khim.*, 2011, **1**, 34-53.
2. W. L. Jorgensen, D. S. Maxwell and J. TiradoRives, *J. Am. Chem. Soc.*, 1996, **118**, 11225-11236.
3. W. L. Jorgensen and J. Tiradorives, *J. Am. Chem. Soc.*, 1988, **110**, 1657-1666.
4. V. S. Neverov and A. V. Komolkin, *J. Chem. Phys.*, 2012, **136**, 094102.
5. P. Ewald, *Ann. Phys.*, 1921, **64** 253-287.
6. J. P. Ryckaert, G. Ciccotti and H. J. C. Berendsen, *J. Comput. Phys.*, 1977, **23**, 327-341.
7. S. Melchionna, *Phys. Rev. E*, 2000, **62**, 5864-5864.
8. W. G. Hoover, *Phys. Rev. A*, 1985, **31**, 1695-1697.

6. Experimental molecular order parameter S in MBBA

Experimental order parameter in nematic MBBA is estimated from the anisotropic contribution $\Delta\delta = \delta_{\text{nem}} - \delta_{\text{iso}}$ to the ^{13}C chemical shifts of the phenyl ring carbons. A semi-empirical correlation

$$S_{ZZ} = \alpha \Delta\delta + \beta$$

has been established for various classes of mesogenic molecules and a database of α , β parameters has been created.¹ Using reported values of the coefficients α and β for MBBA homologous series¹ the S_{ZZ} values were calculated for different carbons in the molecular core as displayed in Table S3. The S_{ZZ} values for different carbons are consistent within the experimental error of ± 0.01 .

Table S3. Order parameters in MBBA at 20°C, calculated from the ^{13}C chemical shift.

Carbon	α	β	$\Delta\delta$, ppm	S_{ZZ}
C1	0,0132	-0,08	48,38	0,559
C2	0,0222	0,17	17,35	0,555
C3	0,0205	0,16	19,47	0,559
C4	0,0070	0,19	53,67	0,566
C1'	0,0082	0,14	50,36	0,553
C2'	0,0189	0,11	23,87	0,561
C3'	0,0224	0,10	20,66	0,563
C4'	0,0085	0,15	47,90	0,557

We have also examined the reported data²⁻¹⁷ for the MBBA molecular order parameter in the literature cited in the database LiqCryst (<https://www.lci-systems.com/liqcryst/>). Reported experimental values for the molecular order parameter in MBBA in the relevant temperature range of 20-25 degrees below clearing temperature T_c , scatter in a wide range of ~ 0.50 - 0.65 (some obvious outliers were excluded). These values are on average significantly below the MD-derived value of $S_{ZZ} = 0.664$. On the other hand, calculated in Table S3 value $S_{ZZ} = 0.56 \pm 0.01$ is well within the reported experimental range. To account for the discrepancy of the modelling and experimental values of the order parameter the couplings obtained from MD trajectory were scaled by a fixed factor $S_{ZZ}^{\text{exp}} / S_{ZZ}^{\text{MD}} \approx 0.85$ (Table S2).

1. T. H. Tong, B. M. Fung and J. P. Bayle, *Liq. Cryst.*, 1997, **22**, 165-169.
2. S. Jen, N. A. Clark and P. S. Pershan, *Phys. Rev. Lett.*, 1973, **31**, 1552-1556.
3. H. S. Subramanyam, C. S. Prabha and D. Krishnamurti, *Mol. Cryst. Liq. Cryst.*, 1974, **28**, 201-215.
4. P. I. Rose, *Mol. Cryst. Liq. Cryst.*, 1974, **26**, 75-85.
5. A. Pines and J. J. Chang, *Phys. Rev. A*, 1974, **10**, 946-949.
6. R. Chang, *Mol. Cryst. Liq. Cryst.*, 1975, **30**, 155-165.
7. K. Miyano, *Phys. Lett. A*, 1977, **63**, 37-38.
8. I. Penchev and I. Dozov, *Phys. Lett. A*, 1977, **60**, 34-36.
9. L. L. Chapoy and D. B. Dupre, *J. Chem. Phys.*, 1979, **70**, 2550-2553.
10. H. Gasparoux, J. R. Lalanne and B. Martin, *Mol. Cryst. Liq. Cryst.*, 1979, **51**, 221-246.
11. P. L. Sherrel and D. A. Crellin, *J. Phys. Colloque (Paris)*, 1979, **40**, C3 211-216.
12. N. Kirov, P. Simova and H. Patajczak, *Mol. Cryst. Liq. Cryst.*, 1980, **58**, 299-310.
13. H. Knepp, V. Reiffenrath and F. Schneider, *Chem. Phys. Lett.*, 1982, **87**, 59-62.

14. I. N. Dozov and I. I. Penchev, *Acta Phys. Pol. A*, 1978, **54**, 649-653.
15. Y. Sasanuma, *J. Phys. II*, 1993, **3**, 1759-1778.
16. R. Y. Dong, L. Friesen and G. M. Richards, *Mol. Phys.*, 1994, **81**, 1017-1038.
17. M. L. Magnuson, B. M. Fung and J. P. Bayle, *Liq. Cryst.*, 1995, **19**, 823-832.